Flatband slow light in photonic crystals featuring spatial pulse compression and terahertz bandwidth

M.D. Settle[1], R.J.P. Engelen[2], M. Salib[3], A. Michaeli[4], L. Kuipers[2] and T.F. Krauss[1]

[1] *School of Physics and Astronomy, St Andrews University, St Andrews, Fife, KY16 9SS, UK*
[2] *Center for Nanophotonics, FOM Institute for Atomic and Molecular Physics (AMOLF), Kruislaan 407, 1098 SJ Amsterdam, The Netherlands*
[3] *Intel Corporation, 2200 Mission College Blvd, Santa Clara, CA 95054 USA*
[4] *Intel Corporation, Kyriat Gat, 82109, Israel*
tfk@st-and.ac.uk

Abstract: Paradoxically, slow light promises to increase the speed of telecommunications in novel photonic structures, such as coupled resonators [1] and photonic crystals [2,3]. Apart from signal delays, the key consequence of slowing light down is the enhancement of light-matter interactions. Linear effects such as refractive index modulation scale linearly with slowdown in photonic crystals [3], and nonlinear effects are expected to scale with its square [4]. By directly observing the spatial compression of an optical pulse, by factor 25, we confirm the mechanism underlying this square scaling law. The key advantage of photonic structures over other slow light concepts is the potentially large bandwidth, which is crucial for telecommunications [5]. Nevertheless, the slow light previously observed in photonic crystals [2,3,6,7] has been very dispersive and featured narrow bandwidth. We demonstrate slow light with a bandwidth of 2.5 THz and a delay-bandwidth product of 30, which is an order of magnitude larger than any reported so far.

OCIS codes: (230.3990) Microstructure devices, (230.7370) Waveguides, (999.9999) Slow light

---

References and links

1. A. Melloni, F. Morichetti and M. Martinelli, "Linear and nonlinear pulse propagation in coupled resonator slow-wave optical structures," Opt. Quantum Electron. **35**, 365-379 (2003).
2. H. Gersen, T.J. Karle, R.J.P. Engelen, W. Bogaerts, J.P. Korterik, N.F. van Hulst, T.F. Krauss and L. Kuipers, "Real-Space Observation of Ultraslow Light in Photonic Crystal Waveguides," Phys. Rev. Lett. **94**, 073903 (2005).
3. Y.A. Vlasov, M. O'Boyle, H.F. Hamann and S.J. McNab, "Active control of slow light on a chip with photonic crystal waveguides," Nature **438**, 65-69 (2005).
4. M. Soljacic and J.D. Joannopoulos, "Enhancement of nonlinear effects using photonic crystals," Nature Materials **3,** 211-219 (2004).
5. J.B. Khurgin, "Optical buffers based on slow light in electromagnetically induced transparent media and coupled resonator structures: comparative analysis," J. Opt. Soc. Am. B **22**, 1062-1074 (2005).
6. M. Notomi, K. Yamada, A. Shinya, J. Takahashi, C. Takahashi and I. Yokohama, "Extremely Large Group-Velocity Dispersion of Line-Defect Waveguides in Photonic Crystal Slabs," Phys. Rev. Lett. **87**, 253902 (2001).
7. R.J.P. Engelen, Y. Sugimoto, Y. Watanabe, J.P. Korterik, N. Ikeda, N. F. van Hulst, K. Asakawa and L. Kuipers, "The effect of higher-order dispersion on slow light propagation in photonic crystal waveguides," Opt. Express **14**, 1658-1672 (2006).
8. M. Settle, M. Salib, A. Michaeli and T.F. Krauss, "Low loss silicon on insulator photonic crystal waveguides made by 193nm optical lithography," Opt. Express **14**, 2440-2245 (2006).
9. Johnson, S. G., & Joannopoulos, J. D., "Block-iterative frequency-domain methods for Maxwell's equations in a planewave," Opt. Express **8**, 173-190, (2001).

10.   M. Notomi, A. Shinya, S. Mitsugi, E. Kuramochi and H-Y Ryu, "Waveguides, resonators and their coupled elements in photonic crystal slabs," Opt. Express **12**, 1551-1561, 2004.
11.   Petrov, A. Yu., & Eich, M., "Zero dispersion at small group velocities in photonic crystal waveguides," Appl. Phys. Lett. **85**, 4866-4868, (2004).
12.   L. H. Frandsen, A. V. Lavrinenko, J. Fage-Pedersen, and P. I. Borel, "Photonic crystal waveguides with semi-slow light and tailored dispersion properties," Opt. Express **14**, 9444-9450 (2006).
13.   M. L. M. Balistreri, H. Gersen, J. P. Korterik, L. Kuipers, N. F. van Hulst, "Tracking Femtosecond Laser Pulses in Space and Time," Science **294**, 1080-1082 (2001).
14.   H. Gersen, T. J. Karle, R. J. P. Engelen, W. Bogaerts, J. P. Korterik, N. F. van Hulst, T. F. Krauss, and L. Kuipers, "Direct Observation of Bloch Harmonics and Negative Phase Velocity in Photonic Crystal Waveguides," Phys. Rev. Lett. **94**, 123901 (2005).
15.   Miyagi, M., Nishida, S., "Pulse spreading in a single-mode fiber due to 3rd-order dispersion," Appl. Opt. **18**, 678-682, (1979).
16.   Hughes, S., Ramunno, L., Young, J.F., & Sipe, J.E., "Extrinsic optical scattering loss in photonic crystal waveguides: role of fabrication disorder and photon group velocity," Phys. Rev. Lett. **94**, 033903, (2005).
17.   Kasapi, A., Jain, M., Jin, G. Y., & Harris, S. E., "EIT: Propagation dynamics," Phys. Rev. Lett. **74**, 2447–2450, (1995).
18.   Ku, P. C., Sedgwich, F., Chang-Hasnain, C., Palinginis, P., Li, T., Wang, H., Chang, S. W., & Chuang, S. L., "Slow light in semiconductor quantum wells," Opt. Lett. **29**, 2291–2293, (2004).
19.   Sharping, J., Okawachi, Y., & Gaeta, A., "Wide bandwidth slow light using a Raman fiber amplifier," Opt. Express **13**, 6092-6098, (2005).
20.   Johnson, S. G., Bienstman, P., Skorobogatiy, M. A., Ibanescu, M., Lidorikis, E., & Joannopoulos, J. D., "Adiabatic theorem and continuous coupled-mode theory for efficient taper transitions in photonic crystals," Phys. Rev. E **66**, 066608, (2002).
21.   Vlasov, Y. A., & McNab, S. J., "Coupling into the slow light mode in slab-type photonic crystal waveguides," Opt. Lett. **31**, 50-52 (2006).

1. Design and fabrication

Our structures are based on a triangular lattice photonic crystal. By removing two rows of holes, a line defect is formed that acts as a waveguide. Since the waveguide is two holes wide, it is referred to as "W2" type. Waveguides were realised in silicon-on-insulator (SOI) material that consists of a 240 nm thick guiding layer on top of 2 µm of SiO_2. They were fabricated on 8-inch wafers using 193 nm deep-UV lithography [8]. Sidewall angles of 87-90° and good etch floors were achieved as shown in Fig. 1.
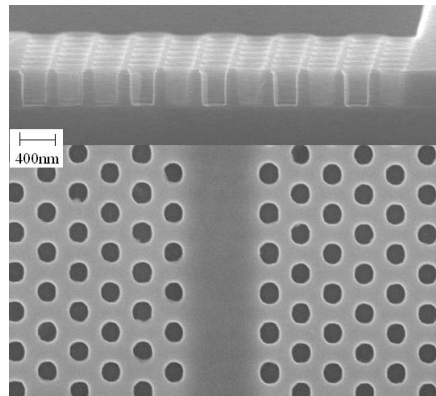

Fig. 1. Top view and cross-section of the W2 waveguide used in the experiments. The lattice period is 420 nm and the hole diameter is 235 nm (r/a=0.28).

Bandstructure calculations were used to establish the required design parameters. First, calculations were performed in 2D using a plane-wave expansion method [9] for a photonic crystal consisting of a triangular lattice with a normalised hole size of r/a = 0.28 and polarisation in the plane of the slab, denoted as TE. We used 1024 plane waves and an effective index of 2.83 for the slab. The resulting bandstructure is shown in Fig. 2. The key

characteristic of a slow mode is its group velocity v_g, which is given by the slope of the dispersion curve in the bandstructure diagram, i.e. $v_g = d\omega/dk$. Two figures of merit are commonly used to describe slow modes, namely the speed of the mode with respect to the speed of light in vacuum c_0, i.e. the group index n_g with $v_g = c_0/n_g$, and the slowdown factor S,

which is defined as the ratio of the phase velocity over the group velocity, $S = v_\phi/v_g$ [1]. S appears to be the better figure of merit given that it focuses on the slow light effect itself by

normalising the group velocity to that obtained in the unstructured material. Note that v_ϕ is to a large extent fixed by the choice of material and waveguide cross-section. Overall, there are four requirements on the slow mode we wish to use, namely a) operation below the light line, b) a "flat" section of the dispersion curve, c) even symmetry and d) single-modedness. Condition (a) is necessary because only modes below the light line are intrinsically loss-less, as those above the light line can couple to radiation modes and are therefore "leaky". Regarding (b), the slope of the dispersion curve of the slow mode should not only be small, but also constant over a given range. Otherwise, the higher order derivatives of the dispersion curve lead to group velocity dispersion and third order dispersion, which distort the signal. The term "flatband" is used to represent this quality. Most of the previous demonstrations of slow light in photonic crystals [2,3,6,7] have violated this condition, although some authors have recognised the importance of adjusting the interplay between bandgap and total internal reflection guiding in order to control higher order dispersion [10-12]. The even symmetry in (c) is needed to facilitate coupling to an incoming waveguide mode, which is typically Gaussian, and d) is required to avoid losses arising from intermode coupling to other modes.
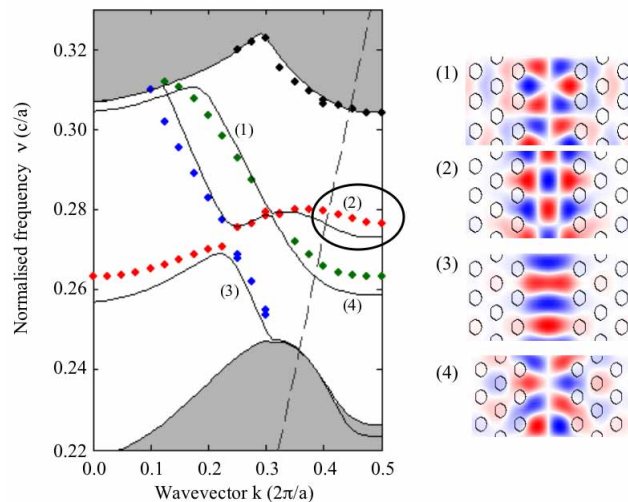

Fig. 2. Comparison of W2 bandstructure calculated by 2D plane wave expansion and 3D FDTD calculation. The mode symmetries are indicated on the left (Hy field components) with the numbers referring to the corresponding points on the bandstructure. Different coloured points in the 3D calculation denote different modes. The light line for the silica cladding is indicated by the dashed diagonal line. The slow light region of interest is highlighted by the oval.

The second order mode highlighted in Fig. 2 comes closest to meeting all of these requirements. Although it is not the only mode available in the frequency range around 0.27 c/a, our measurements confirm that it is a low-loss mode, so intermode coupling losses appear low and violating condition (d) seems to have little consequence. What is particularly noteworthy is that in the regime below the light line, i.e. between k=0.4 and 0.45, it features a low group velocity as well as appearing rather straight, thus indicating low dispersion. In order to confirm these properties, we conducted 3D bandstructure calculations using the RSoft FULLWAVE code with a grid size of λ/20. The result of these calculations, shown by the dots in Fig. 2, yielded a surprise. While there was a good match in the centre region for a

frequency of 0.27 (wavelength of 1.55 µm), the bands deviated significantly elsewhere, especially in the slow light regime. Please note that, since the 3D calculation agrees very well with the measurement (Fig. 3), the assumptions used in the 2D calculation must be the reason for this deviation. Slow modes cannot be thought of as purely planar modes in the slab, i.e. they travel at "skewed" angles in the ray-optics picture. Therefore, they can no longer be considered purely "TE" or "TM" and will therefore not be accurately described by the idealised 2D bandstructure. 3D analysis therefore provides a much better representation of these modes, which is confirmed by Fig 3. 3D analysis also indicates the presence of a very flatband regime below the lightline. Especially the portion of the band between k=0.40 and k=0.45 appears to be very straight with little curvature. This section should therefore yield slow light with low dispersion, i.e. "flatband slow light", which is the desired characteristic. The group velocity of the mode from the bandstructure is c/25, which corresponds to a slowdown factor of approximately 12 given the effective (phase) index of n_ϕ=2.14 in the waveguide. This phase index can be directly determined from the unfolded bandstructure, e.g. at point k=0.6, ν=0.28, and is different from the phase index used to approximate the slab in the 2D calculation since it is specific to each photonic crystal mode.

2. Characterisation

Devices were characterised with a tuneable continuous wave laser in the wavelength range from 1440 nm-1592 nm. This corresponds to a frequency range of 0.264-0.292 c/a for a lattice constant *a* of 420 nm. A phase-sensitive scanning near field optical microscope (PSNOM) [13] was used to map the electric-field distribution of the light in the waveguide. These E-field maps contain both the amplitude and the phase of the field. The wavevector of the light can then be recovered by a Fourier transformation of the field distribution measured at each optical frequency ω.
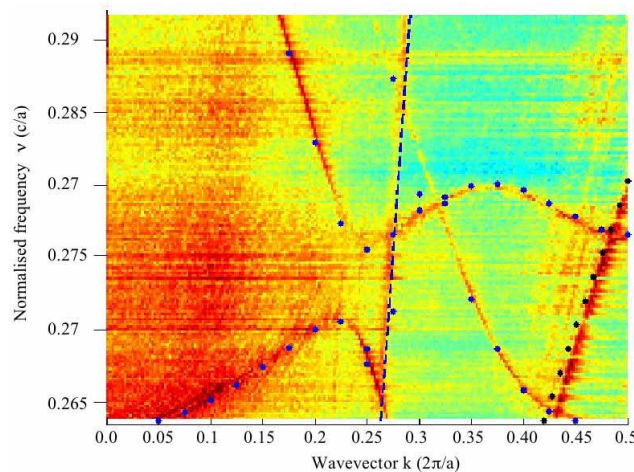

Fig. 3. Bandstructure obtained by PSNOM measurement with 3D FDTD calculation overlaid. The FDTD points for the TE mode (blue dots) are identical to those shown in Fig. 2 and show very good agreement with the measured data. The TM mode (black dots) can be identified at k>0.43 2π/a by the fact that it has a weak interaction with the photonic crystal lattice, and therefore does not show a clear stopband at the Brillouin zone band-edge, i.e. it appears as a straight diagonal line. The dashed line represents the light line for air.

In this way, we reconstructed the bandstructure (ν,*k*) of the W2 waveguide [14]. Fig. 3 shows the resulting bandstructure, with the 3D FDTD points of Fig. 2 overlaid. The TE bands show perfect agreement, but there is also clear evidence for TM modes (magnetic field in the plane of the slab). These are excited because of the asymmetric cladding (SiO$_2$ bottom cladding, air above), which means that TE and TM modes are not truly orthogonal and can therefore interact.

In order to study the slowdown factor, propagation loss, pulse compression and dispersion in the slow light regime, we injected femtosecond pulses into the waveguide. Pulses were centred at 1509 nm (ν=0.278 c/a) and had a FWHM of 22 nm, slightly exceeding the bandwidth of the slow 2nd order mode below the light line. Using our near-field microscope, we tracked the pulses as they propagated through the waveguide. The resulting pulse evolution is shown in Fig. 4 (a), which shows the amplitude of the pulse along the waveguide (each vertical line representing a pulse and thereby its position in the waveguide) as a function of time (horizontal axis). We can clearly distinguish two dominant modes, namely a relatively "fast" mode, identified as the zero order TM in fig. 3, and the slow mode of interest. A simple comparison between these two modes can be used to assign a delay time-bandwidth product; while the fast mode takes 4 ps to traverse the 160μm long waveguide, the slow mode takes 16 ps. The difference of 12 ps, multiplied by the bandwidth of 2.5 THz, yields the product of 30. This is by far the largest time-bandwidth product of any slow light system demonstrated so far, as further discussed in table 2 below.
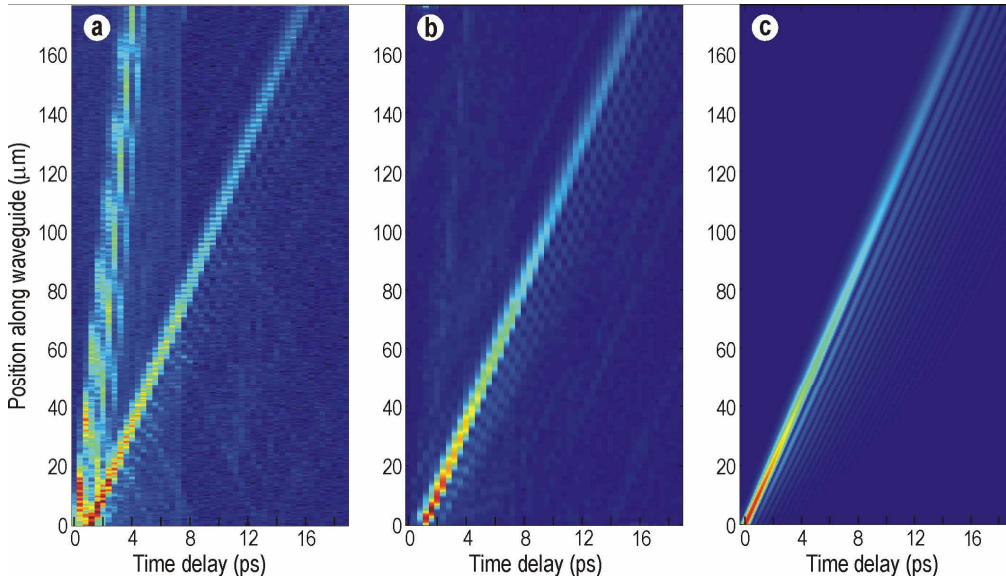

Fig. 4. Tracing pulse propagation in the slow mode with fs pulses. (a) Experimental result of tracing the pulses propagating in the waveguide. (b) Experimental result obtained by Fourier filtering the slow mode. The Fourier filtering highlights the properties of the slow mode (c) Simulated pulse propagation derived from the dispersion curve for comparison with (b).

The same picture was then also Fourier filtered in order to highlight the properties of the slow mode in Fig. 4(b). The data was first Fourier transformed to yield all the wavevectors present. The forward propagating wavevectors in the range of the slow mode 0.37<|k|<0.5 were then selectively backtransformed to obtain only the slow mode and to allow its study in more detail. For comparison, we also used the measured bandstructure in Fig. 3 to simulate the propagation of a pulse. This can be seen in Fig. 4(c), where the pulse amplitude is depicted as a function of waveguide position and time, in the same way as the experiment in Fig. 4(b). From both images, we can make several important observations. First of all, the pulse does not appear to broaden significantly, i.e. the main lobe maintains its apparent size over the length of the waveguide. However, side-lobes appear on the trailing edge of the pulse. These side-lobes are in part due to the limited bandwidth of the slow mode (19 nm compared to 22 nm FWHM of the pulse) but mainly due to higher order dispersion [7], an effect that is known to occur in third-order-dispersive media [15]. In order to match the observed decay of the peak of the main lobe in Figs 4(a) and 4(b), we included a loss coefficient 244 dB/cm into the modelled result (Fig. 4(c)). At first sight, this appears rather higher than expected and compares unfavourably against the best reported loss in comparable single line defect ("W1")

waveguides of 14 dB/cm [8]. If we scale the loss linearly with the slowdown factor S=12, however, we obtain a value of 244/12=20 dB/cm. This only differs by a factor of 1.4 from the best result obtained for a "fast" mode, which can be explained by the intermode coupling discussed previously. While this analysis is only indicative, given that different types of waveguide are being compared and we cannot easily distinguish the different sources of loss, it does suggest that linear scaling is the most likely functional dependence of the loss on slowdown factor. The inverse square scaling of the loss with group velocity suggested by other authors [16] therefore appears exaggerated.

We can also derive the group velocity of the pulse, its compression factor and dispersion. The group velocity is estimated by fitting a straight line through the maxima of the pulses, which yields a value of v_g =c/25 . Pulse compression results from the fact that a pulse of a given duration propagating in a slow light medium will be compressed in space, and this is indeed what we observe with surprising precision. Near the entrance of the waveguide, we observe a pulselength of 6.8 µm (Fig. 5), which compares to the pulselength of 167 µm of a comparable pulse in free space. The corresponding compression factor of 167/6.8=24.5 closely matches the observed reduction of the group velocity by a factor 25.
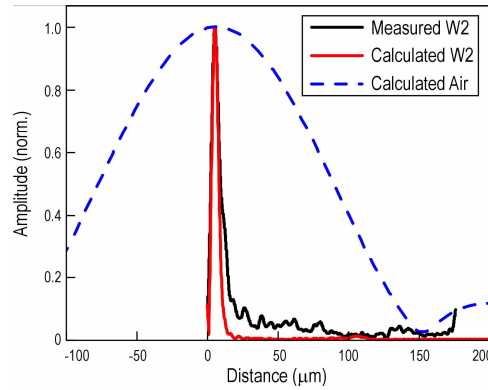

Fig.5. Slow pulse propagating near the entrance of the W2 waveguide, highlighting the compression from 167 µm for the equivalent cut-off spectrum down to 6.8 µm for the measured spectrum.

The slight broadening of the pulse along the 160 µm long waveguide (Fig. 4) can be explained with dispersive broadening. In order to quantify this, we can derive values for the second and third order dispersion from our measured bandstructure. These are summarised in table 1 and show that both the second and third order dispersion is reduced by an order of magnitude compared to a W1, while maintaining the same group velocity reduction.

Table 1. Comparison of second and third order dispersion in W1 and W2 waveguides. Data for W1 waveguides are derived from [7].

	Group index	k-point [$2\pi/a$]	GVD [ps^2/km]	TOD [ps^3/km]
W1 [7]	25	0.383	1.73×10^7	7.94×10^6
W2 [This work]	25	0.431	1.86×10^6	1.14×10^6

This reduced dispersion is the main reason why in a W2, the slow light compression dominates over dispersive broadening as already highlighted in Fig. 5. The fact that third-order dispersion is nonzero also explains the fringes observed in Fig. 4.

3. Discussion and conclusion

The slowdown factor S forms a powerful addition to the photonic circuit designer's toolkit: Due to the increased interaction time, linear effects such as gain and refractive index modulation scale linearly with S, yielding low power switches and modulators [3], whereas nonlinear effects are expected to scale with S^2 [4]. The physical mechanism behind this additional enhancement of nonlinear effects is the spatial compression of a light pulse, which leads to an increase in its energy per unit volume. By demonstrating pulse compression in close agreement with the reduction in group velocity, we have verified this favourable scaling law. This means that low power all-optical switches and modulators based on slow light are indeed a realistic prospect. For example, the slowdown factor of S=12 demonstrated here would yield a switching power reduction by over two orders of magnitude. Please note that this scaling law only applies to dielectric slow light structures; in slow light structures based on atomic resonances, the energy is transferred instead to electronic excitations of the medium rather than leading to an increase of the energy density of the mode.

These benefits can only be exploited, however, if the bandwidth of the slow light structure exceeds the bandwidth of the signal. This is of particular concern if slow light structures are to be used in future all-optical networks that are likely to operate at bandwidths well in excess of 100 GHz. Even though slowdown factors much exceeding the moderate value of S=12 reported here have been demonstrated in other systems, none have been able to realise the large bandwidth or bandwidth–delay product we have achieved (table 2).

Table 2. Comparison of a range of slow light systems.

System/parameter	Slowdown factor $S=v\phi/vg$	Bandwidth B	Observed delay	Delay-bandwidth product	Tuning
Pb [17]	165	30 MHz	55 ns	1.7	dynamic
Population oscillations [18]	~10k	2 GHz	<1ns	<1	dynamic
Stimulated Raman scattering [19]	~1	1 THz	370 fs	0.4	dynamic
This work	12	2.5 THz	12 ps*	30	static

* Taken as the delay difference between the fast mode and the slow mode in Fig. 4 (a).

Rather than pursuing large slowdown factors irrespective of bandwidth, it is then much more prudent to balance bandwidth with slowdown factor. In the photonic crystal system, this can be done within the restriction imposed by the size of the Brillouin zone and the light line limitation. Increased slowdown factors therefore occur at the expense of reduced bandwidth, but slowdown factors of 20-30 will clearly be possible with bandwidths exceeding 500 GHz. Furthermore, the photonic crystal system as presented here is static, i.e. there is no easy tuning mechanism for the slowdown factor available. This indicates that the photonic crystal approach is more suitable for applications in low power switches, modulators and nonlinear devices rather than tuneable delay or optical memory.

Another issue for slow light devices is waveguide dispersion, as already demonstrated by the dispersive broadening observed in W1 waveguides [7]. Our W2 design shows improvements of an order of magnitude or more in terms of both second and third-order dispersion compared to a standard W1, and we believe that this can be pushed further by more sophisticated designs altering the waveguide parameters, such as individual hole size and waveguide width [11,12]. While highlighting the potential of the "flatband slow light" concept, this also emphasizes the need to design structures appropriately rather than operating on the typically parabolic bands occurring near the band-edge of a periodic structure.

In order to improve the device further and fully exploit the slow light regime, efficient couplers need to be designed that allow efficient and broadband injection into slow modes. Several schemes have been suggested, e.g. the use of adiabatic transitions [20]; also, the importance of the termination has been pointed out [21]. Neither of these schemes were implemented in the present device and the design needs to be refined accordingly. Furthermore, it is desirable to develop a design capable of single-mode operation, which can be realised by reducing the waveguide width. Despite these obvious improvements, the present scheme has clearly shown the powerful possibilities available with photonic crystals that operate in the slow light regime.

Acknowledgments